Journal of Sound and Vibration 333 (2014) 4444–4457

Contents lists available at ScienceDirect

Journal of Sound and Vibration

journal homepage: www.elsevier.com/locate/jsvi

Nonlinear vibration control and energy harvesting of a beam using a nonlinear energy sink and a piezoelectric device

Z. Nili Ahmadabadi [a,*], S.E. Khadem [b]

[a] Department of Mechanical Engineering, École de Technologie Supérieure, 1100 rue Notre-Dame Ouest, Montréal, Québec, Canada H3C1K3
[b] Department of Mechanical Engineering, Tarbiat Modares University, P.O. Box 14115-177, Tehran, Iran

ARTICLE INFO

Article history:
Received 16 June 2013
Received in revised form
14 April 2014
Accepted 14 April 2014
Handling Editor: W. Lacarbonara
Available online 27 May 2014

ABSTRACT

This paper presents an optimal design for a system comprising a nonlinear energy sink (NES) and a piezoelectric-based vibration energy harvester attached to a free–free beam under shock excitation. The energy harvester is used for scavenging vibration energy dissipated by the NES. Grounded and ungrounded configurations are examined and the systems parameters are optimized globally to both maximize the dissipated energy by the NES and increase the harvested energy by piezoelectric element. A satisfactory amount of energy has been harvested as electric power in both configurations. The realization of nonlinear vibration control through one-way irreversible nonlinear energy pumping and optimizing the system parameters result in acquiring up to 78 percent dissipation of the grounded system energy.

1. Introduction

Great attention has been recently paid to employing nonlinear energy sink as an essential nonlinear vibration absorber rather than tuned-mass-damper linear absorber or weakly nonlinear absorber.

Application of the NES in two degrees-of-freedom (dof) or multi dof systems of weakly coupled linear and essentially nonlinear damped oscillators with different parameters and conditions were studied in several works [1–6] widely for nonlinear energy pumping and a variety of system response regimes such as strongly modulated responses (SMRs). However, the existence of nonlinearities in systems containing NES causes additional branches of periodic regimes which might interfere with the energy absorption. Refs [7,8] employ a NES with nonlinear damping characteristics to annihilate these undesired periodic response regimes and simultaneously preserve SMR in a harmonically excited one and two dof oscillatory systems, respectively.

The NES can also be of use in suppression of self-excited oscillations in the drill string system [9,10]. It was demonstrated in [9] that attaching NES to different components of a drill string would help to acquire better responses and/or to improve applicability of the NES.

Passive targeted energy transfer in discrete systems of coupled oscillators is not the only usage of the NES. In [11], the authors showed that the NES can successfully absorb and dissipate energy in linear continuous systems such as beams. Then ref. [12] studied the bifurcations and topological structure of nonlinear normal modes of a system consisting of a cantilever beam and an attached/coupled NES in order to find the necessary conditions of targeted energy transfer (TET) realization.

* Corresponding author. Tel.: +1 514 5139349.
E-mail address: zahra.nili-ahmadabadi.1@ens.etsmtl.ca (Z. Nili Ahmadabadi).

http://dx.doi.org/10.1016/j.jsv.2014.04.033
0022-460X/

So far, the NES has been successfully applied in many various mechanical systems to absorb and dissipate undesired vibration energy. However, harvesting the dissipated energy by the NES damper has not yet been investigated. This dissipated energy could be very significant in some cases that make energy harvesting economically efficient.

Over the past few years, the use of piezoelectric elements for harvesting the mechanical vibration energy has attracted a growing interest due to their capability of electromechanical conversion. A great number of papers studied power harvesting from vibration using piezoelectric materials and proposed their precise models [13–22]. Sodano et al. [20] developed a model to predict the amount of generated power through the vibration of a cantilever beam with attached piezoelectric elements. In order to maximize harvested power from a vibrating structure, Cornwell et al. [13] applied a tuned auxiliary structure consisting of a mechanical fixture and a piezoelectric element. Lefeuvre et al. [15] presented four vibration-powered generators designed to power standalone systems, such as wireless transducers. The proposed approaches were based on a particular processing of the voltage delivered by the piezoelectric material, which enhanced the electromechanical conversion. Stephen [21] analyzed the extraction of energy from a vibrating environment and concluded that for both direct mass (force) and base excitations, the maximum power flow into the device depends on the frequency and the amplitude of force (or the base) and the size of the device. Beeby et al. [18] designed a small micro electromagnetic generator and optimized it for a low ambient vibration level. Sodano and Inman [23] reviewed in detail the research in the area of power harvesting from vibration.

The present paper is an attempt to apply a piezoelectric device to capture and store the dissipated energy by the NES. The system's parameters are optimized to both maximize the dissipated energy by the NES and increase the harvested energy by the piezoelectric element. Two different configurations are examined by attaching one piezoelectric element and one NES to the primary system of a free–free beam under shock excitation.

Here, the free–free beam represents a flying object. Many important mechanical, aerospace and naval structures such as aircrafts, missiles, rockets, and ships can be mathematically modeled by a free–free beam. Recently, the free–free beams have also been used as micromechanical resonators [24]. In fact the main purpose in choosing the free–free beam as the primary system is to study the applicability of the NES in dealing with the structures with no supports along their length.

2. Energy harvesting using piezoelectric device

2.1. Electromechanical model

Energy absorbed by the NES can be harvested using an electromechanical device. This section first presents a concise introduction about modeling of the electromechanical system consisting of piezoelectric element and mass–spring–damper absorber. In order to convert sufficient amount of energy, the corresponding deformation of the piezoelectric material should be large enough. In fact under the conditions that the piezoelectric generator is optimized to work around the resonance frequency and the displacement of mechanical structure is small enough to consider the motion as linear, electrical behavior of a structure with piezoelectric element can be simply modeled as a mass–piezo–spring–damper system with a single degree of freedom, as shown in Fig. 1.

In this model, M represents the rigid mass, C is the viscous damper which shows mechanical losses of the structure, k is the stiffness of the mechanical structure, u is the rigid mass displacement, F is the driving force, I is the outgoing current, and V is the voltage of the piezoelectric elements. The piezoelectric equations can be expressed as:

$$F_p = k_p u + \alpha V\,, \tag{1a}$$

$$I_p = \alpha u - C_p V \tag{1b}$$

where k_p is the equivalent stiffness of the piezoelectric layer when it is short-circuited; α is the force factor; C_p is the clamped capacitance of the piezoelectric elements; and F_p represents the driving force.

The governing equation of the model is given by:

$$M\ddot{u} + c\dot{u} + ku^3 + F_p = F \tag{2}$$

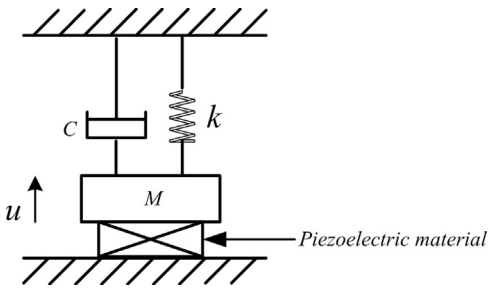

Fig. 1. Model of an absorber with piezoelectric element.

Substituting Eq. (1a) into Eq. (2) and knowing that $V = C_p^{-1} I_p$, one may have:

$$M\ddot{u} + c\dot{u} + k_p u + ku^3 + \alpha C_p^{-1} I_p = F \tag{3}$$

The output voltage V can also be expressed in terms of load resistance R as:

$$V = R\dot{I}_p$$

So replacing this relation into Eq. (1b) yields:

$$R\dot{I}_p - C_p^{-1}\alpha u + C_p^{-1} I_p = 0 \tag{4}$$

Solving Eqs. (3) and (4) results in electrical response of the system.

2.2. Dynamical model and optimization approach

Consider a free–free beam which is attached to a NES and a piezoelectric element. The NES is comprised of a nonlinear spring with essential cubic nonlinearity, a relatively small mass, and a linear viscous damper. The piezoelectric element is intended to harvest the energy dissipated by the NES. Two main different configurations shown in Fig. 2 would be examined: grounded and ungrounded. In the grounded configuration, piezoelectric element is between the NES mass and the ground, while in the ungrounded configuration it is located between the NES mass and the beam.

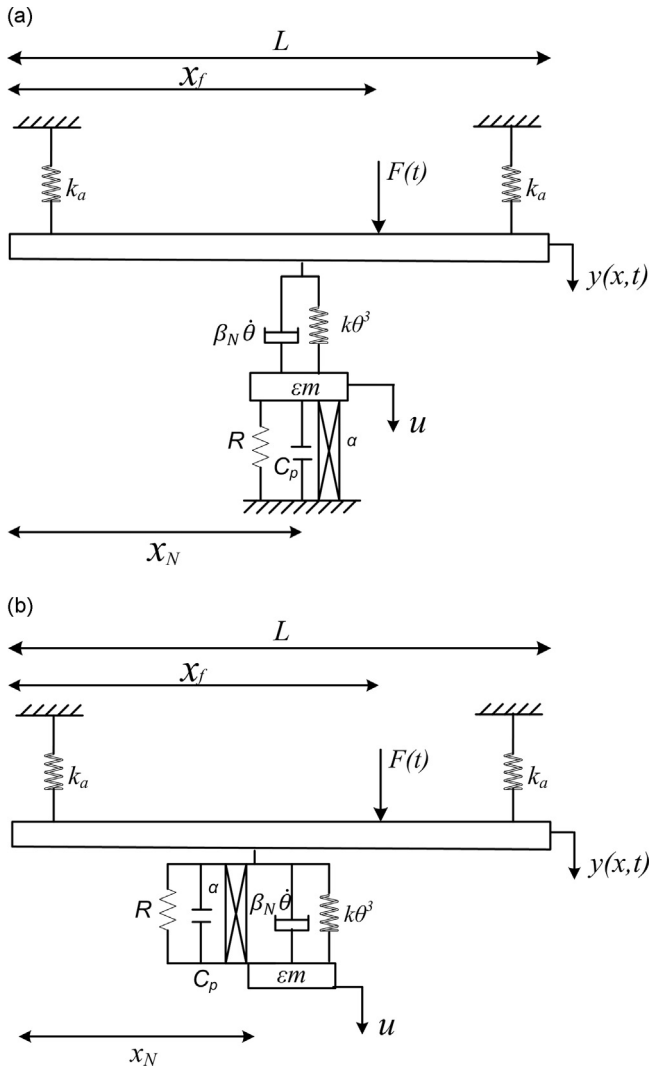

Fig. 2. NES configurations: (a) Configuration#1, (b) Configuration#2.

Applying the Euler–Bernoulli beam theory, the equations of motion for the two configurations would be in the following forms: Grounded configuration, Configuration#1,

$$E_B I\frac{\partial^4 y}{\partial x^4}+M\frac{\partial^2 y}{\partial t^2}+\varepsilon\beta_1\frac{\partial y}{\partial t}+k_a y\left(\frac{L}{8},t\right)\delta\left(x-\frac{L}{8}\right)+k_a y\left(\frac{7L}{8},t\right)\delta\left(x-\frac{7L}{8}\right)$$
$$+\{\varepsilon k[y(x_N,t)-u(t)]^3+\varepsilon\beta_N[\dot{y}(x_N,t)-\dot{u}(t)]\}\delta(x-x_N)=F(t)\delta(x-x_f)$$
$$\times\varepsilon m\,\ddot{u}(t)+\varepsilon k[u(t)-y(x_N,t)]^3+\varepsilon\beta_N[\dot{u}(t)-\dot{y}(x_N,t)]+k_p u(t)-\frac{\alpha}{C_p}I(t)=0$$
$$R\dot{I}(t)-\frac{\alpha}{C_p}u(t)+\frac{I(t)}{C_p}=0 \tag{5}$$

Table 1
Corresponding values of b_f, b_s, and βL for each mode.

Mode number	βL	b_f	b_s
0	0	1.00	0
1	0	1.00	0
2	4.73	1.00	3500.56
3	7.85	0.99	3803.846
4	10.996	1.00	15014.402

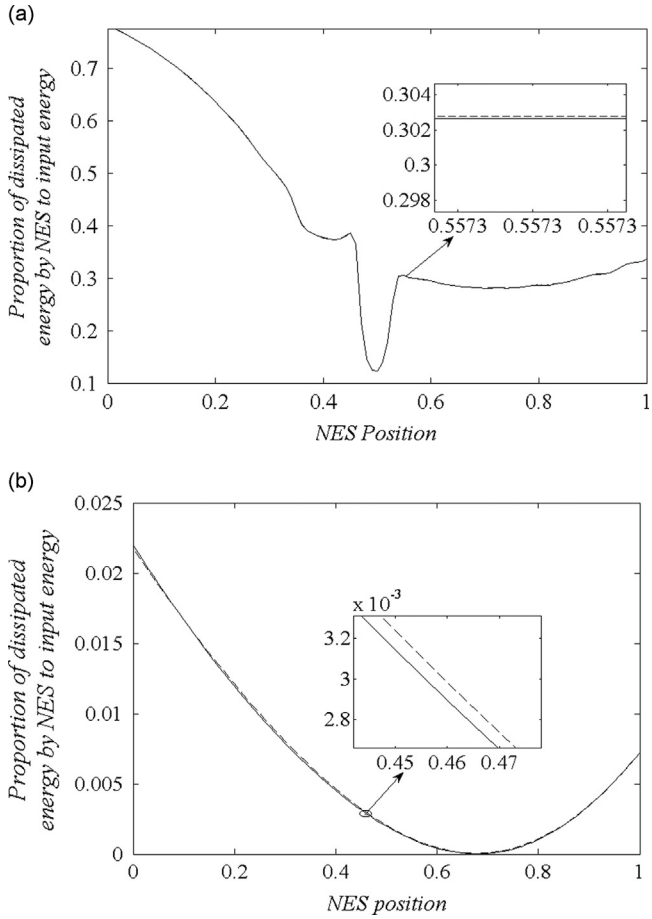

Fig. 3. Input energy dissipated by the NES as a function of the NES spring stiffness for a shortened system with 3 and 5 modes ($m=1.06$, $\beta_N=0.47$, $C_p=8.9\text{e}-6$, $\alpha=0.027$, $R=1.1\text{e}+4$, $\varepsilon=0.1$, $A=10$, $T=0.4/\pi$, $E_BI=291.69$, $M=1.35$, $\beta_1=0.5$, $k_a=1$, $x_f=0$): (a) Configuration#1 for $k=100$, $k_p=500$, and (b) Configuration#2 for $k=420$, $k_p=380$. Solid line: 3 modes; dashed line: 5 modes.

Ungrounded configuration, Configuration#2,

$$E_B I\frac{\partial^4 y}{\partial x^4}+M\frac{\partial^2 y}{\partial t^2}+\varepsilon\beta_1\frac{\partial y}{\partial t}+k_a y\left(\frac{L}{8},t\right)\delta\left(x-\frac{L}{8}\right)+k_a y\left(\frac{7L}{8},t\right)\delta\left(x-\frac{7L}{8}\right)$$

$$+\{\varepsilon k[y(x_N,t)-u(t)]^3+\varepsilon\beta_N[\dot{y}(x_N,t)-\dot{u}(t)]\}\delta(x-x_N)=F(t)\delta(x-x_f)$$

$$\times\varepsilon m\ \ddot{u}(t)+\varepsilon k[u(t)-y(x_N,t)]^3+\varepsilon\beta_N[\dot{u}(t)-\dot{y}(x_N,t)]+k_p\ [u(t)-y(x_N,t)]-\frac{\alpha}{C_p}I(t)=0$$

$$R\dot{I}(t)-\frac{\alpha}{C_p}[u(t)-y(x_N,t)]+\frac{I(t)}{C_p}=0 \tag{6}$$

where the dot denotes the differentiation with respect to t; $y=y(x,t)$ is the transverse displacement of the beam; E_BI is the bending stiffness of the beam; M is the beam mass per unit length; k_a and k are the coupling spring stiffness and the spring stiffness of the NES, respectively; β_1 and β_N are the damping coefficients of the beam and the NES, respectively; m is the NES mass; $F(t)$ is the external shock load; x_f and x_N are the places of applying the external load and attaching the NES (and piezoelectric element); L is the length of the beam; $\delta(x)$ is the Dirac function; $\varepsilon \ll 1$.

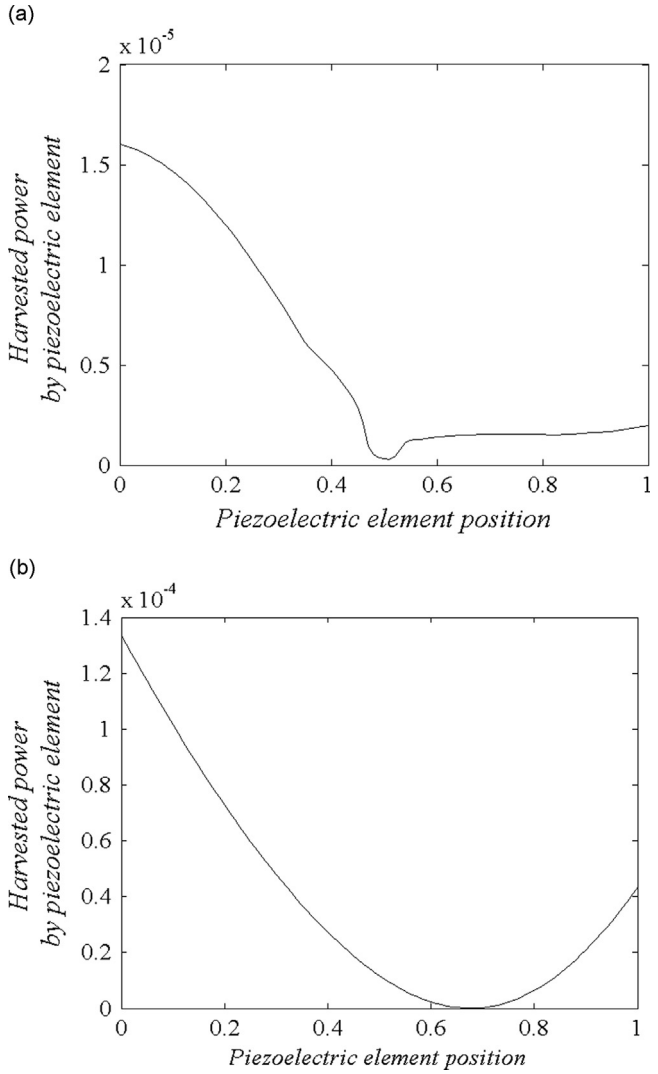

Fig. 4. Harvested power by the piezoelectric element ($m=1.06$, $\beta_N=0.47$, $C_p=8.9\text{e}-6$, $\alpha=0.027$, $R=1.1\text{e}+4$, $\varepsilon=0.1$, $A=10$, $T=0.4/\pi$, $E_BI=291.69$, $M=1.35$, $\beta_1=0.5$, $k_a=1$, $x_f=0$): (a) Configuration#1 for $k=100$, $k_p=500$, and (b) Configuration#2 for $k=420$, $k_p=380$.

The nth vibration mode Φ_n and frequency ω_n of a free–free beam are

$$\Phi_0(x)=1, \quad \Phi_1(x)=A_1\left(x-\frac{L}{2}\right),$$

$$\Phi_n(x)=A_n\{[\cosh(\beta_n L)-\cos(\beta_n L)][(\sin(\beta_n x)+\sinh(\beta_n x))]$$

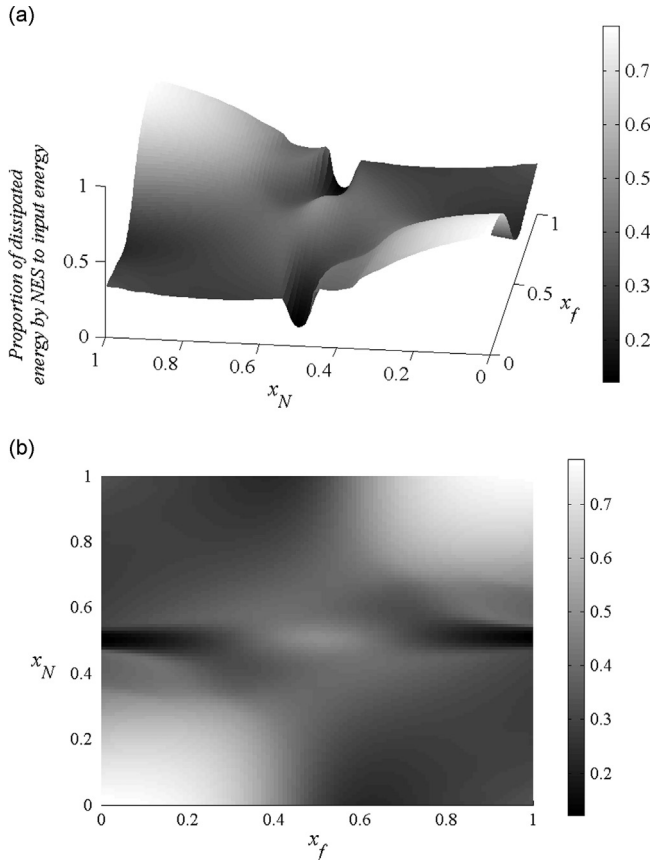

Fig. 5. Input energy dissipated by the NES in Configuration#1 as a function of the NES position and position of load application ($m=1.06$, $\beta_N=0.47$, $C_p=8.9\text{e}-6$, $\alpha=0.027$, $R=1.1\text{e}+4$, $\varepsilon=0.1$, $A=10$, $T=0.4/\pi$, $E_BI=291.69$, $M=1.35$, $\beta_1=0.5$, $k_a=1$, $k=100$, $k_p=500$): (a) three-dimensional plot, (b) contour projection in the (x_f, x_N) plane.

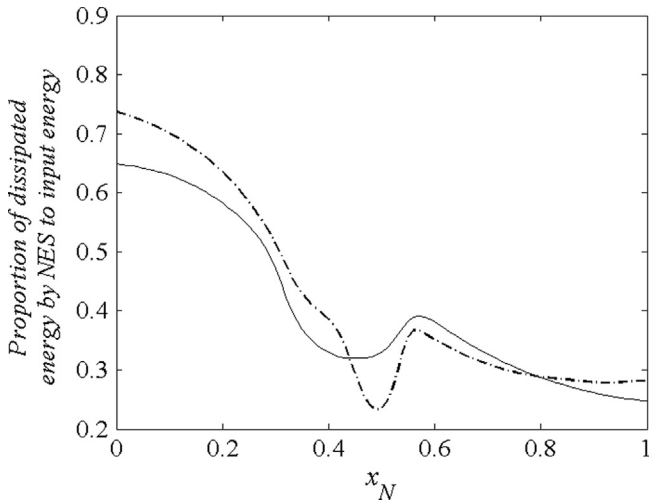

Fig. 6. Input energy dissipated by the NES in Configuration#1 as a function of the NES position ($m=1.06$, $\beta_N=0.47$, $C_p=8.9\text{e}-6$, $\alpha=0.027$, $R=1.1\text{e}+4$, $\varepsilon=0.1$, $A=10$, $T=0.4/\pi$, $E_BI=291.69$, $M=1.35$, $\beta_1=0.5$, $k_a=1$, $k=100$, $k_p=500$). Dash-dot line: $x_f=0.2$; solid line: $x_f=0.3$.

$$+[\sin(\beta_n L) - \sinh(\beta_n L)][(\cos(\beta_n x) + \cosh(\beta_n x))]\} \qquad n = 2, \ldots, \infty$$

$$\omega_n = \beta_n^2 \sqrt{\frac{E_B I}{M}}$$

$$A_n = \left\{ \int_{x=0}^{L} M \left[\frac{\Phi_n(x)}{A_n} \right]^2 dx \right\}^{-1/2} \tag{7}$$

Here, A_n is the amplitude of the beam vibration. β_n will be obtained by solving the following equation:

$$\beta_0 = 0,$$
$$\cos(\beta_n L)\cos\ h(\beta_n L) = 1, \quad n = 1, \ldots, \infty$$

Using the Galerkin method, the beam displacement can be expressed as

$$y(x,t) = \sum_{n=0}^{\infty} q_n(t)\Phi_n(x) \tag{8}$$

The orthonormality condition is given by

$$\int_0^L M\Phi_i(z)\Phi_j(z)\, dz = \delta_{ij} \quad i,j = 0,1,2,\ldots \tag{9}$$

Thus using Eqs. (8) and (9), one obtains:
Configuration#1,

$$Mb_{fp}\ddot{q}_p(t) + \varepsilon\beta_1 b_{fp}\dot{q}_p(t) + E_B I b_{sp} q_p(t) + k_a\left[\sum_{r=0}^{\infty} q_r(t)\Phi_r\left(\frac{L}{8}\right)\right]\Phi_p\left(\frac{L}{8}\right) + k_a\left[\sum_{r=0}^{\infty} q_r(t)\Phi_r\left(\frac{7L}{8}\right)\right]\Phi_p\left(\frac{7L}{8}\right)$$
$$+\left\{\varepsilon k\left[\sum_{r=0}^{\infty} q_r(t)\Phi_r(x_N) - u(t)\right]^3 + \varepsilon\beta_N\left[\sum_{r=0}^{\infty}\dot{q}_r(t)\Phi_r(x_N) - \dot{u}(t)\right]\right\}\Phi_p(x_N) = F(t)\Phi_p(x_f) \quad p = 0,\ldots,\infty$$
$$\varepsilon m\ \ddot{u}(t) + \varepsilon k\left[u(t) - \sum_{r=0}^{\infty} q_r(t)\Phi_r(x_N)\right]^3 + \varepsilon\beta_N\left[\dot{u}(t) - \sum_{r=0}^{\infty}\dot{q}_r(t)\Phi_r(x_N)\right] + k_p u(t) - \frac{\alpha}{C_p} I(t) = 0$$
$$R\dot{I}(t) - \frac{\alpha}{C_p}u(t) + \frac{I(t)}{C_p} = 0 \tag{10}$$

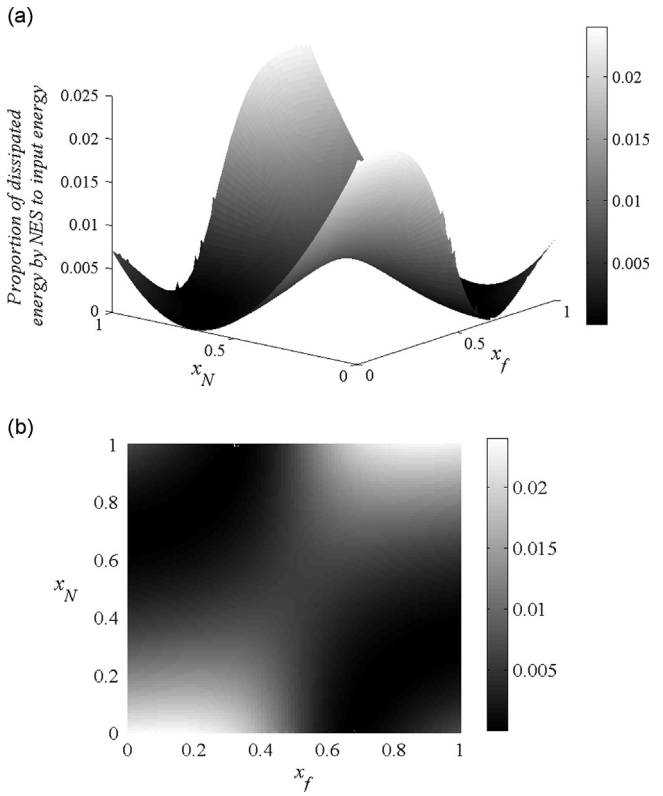

Fig. 7. Input energy dissipated by the NES in Configuration#2 as a function of the NES position and position of load application ($m = 1.06$, $\beta_N = 0.47$, $C_p = 8.9\text{e}{-6}$, $\alpha = 0.027$, $R = 1.1\text{e}{+4}$, $\varepsilon = 0.1$, $A = 10$, $T = 0.4/\pi$, $E_B I = 291.69$, $M = 1.35$, $\beta_1 = 0.5$, $k_a = 1$, $k = 420$, $k_p = 380$): (a) three-dimensional plot, (b) contour projection in the (x_f, x_N) plane.

Configuration♯2,

$$Mb_{fp}\ddot{q}_p(t)+\varepsilon\beta_1 b_{fp}\dot{q}_p(t)+E_BIb_{sp}q_p(t)+k_a\left[\sum_{r=0}^{\infty}q_r(t)\Phi_r\left(\frac{L}{8}\right)\right]\Phi_p\left(\frac{L}{8}\right)+k_a\left[\sum_{r=0}^{\infty}q_r(t)\Phi_r\left(\frac{7L}{8}\right)\right]\Phi_p\left(\frac{7L}{8}\right)$$
$$+\left\{\varepsilon k\left[\sum_{r=0}^{\infty}q_r(t)\Phi_r(x_N)-u(t)\right]^3+\varepsilon\beta_N\left[\sum_{r=0}^{\infty}\dot{q}_r(t)\Phi_r(x_N)-\dot{u}(t)\right]\right\}\Phi_p(x_N)=F(t)\Phi_p(x_f)\qquad p=0,\ldots,\infty$$
$$\varepsilon m\ \ddot{u}(t)+\varepsilon k\left[u(t)-\sum_{r=0}^{\infty}q_r(t)\Phi_r(x_N)\right]^3+\varepsilon\beta_N\left[\dot{u}(t)-\sum_{r=0}^{\infty}\dot{q}_r(t)\Phi_r(x_N)\right]+k_p\left[u(t)-\sum_{r=0}^{\infty}q_r(t)\Phi_r(x_N)\right]-\frac{\alpha}{C_p}I(t)=0$$
$$R\dot{I}(t)-\frac{\alpha}{C_p}\left[u(t)-\sum_{r=0}^{\infty}q_r(t)\Phi_r(x_N)\right]+\frac{I(t)}{C_p}=0 \tag{11}$$

where

$$b_{fp}=\int_{x=0}^{L}\Phi_p^2(x)\mathrm{d}x$$
$$b_{sp}=\int_{x=0}^{L}\frac{\mathrm{d}^4\Phi_p(x)}{\mathrm{d}x^4}\Phi_p(x)\mathrm{d}x$$

Values of b_f, b_s, and βL for each mode are shown in Table 1.

The input load is a shock load applied at $x=x_f$ (as shown in Fig. 2). This load can be expressed in the following form:

$$F(\tau)=\mathrm{A}\ \mathrm{Heaviside}\left(\frac{T}{2}-\tau\right)\sin\left(\frac{2\pi\tau}{T}\right) \tag{12}$$

In order to maximize energy dissipation in the NES and optimize harvested energy by the piezoelectric element, an optimized set of electrical and mechanical parameters should be obtained for each configuration. Dynamic optimization

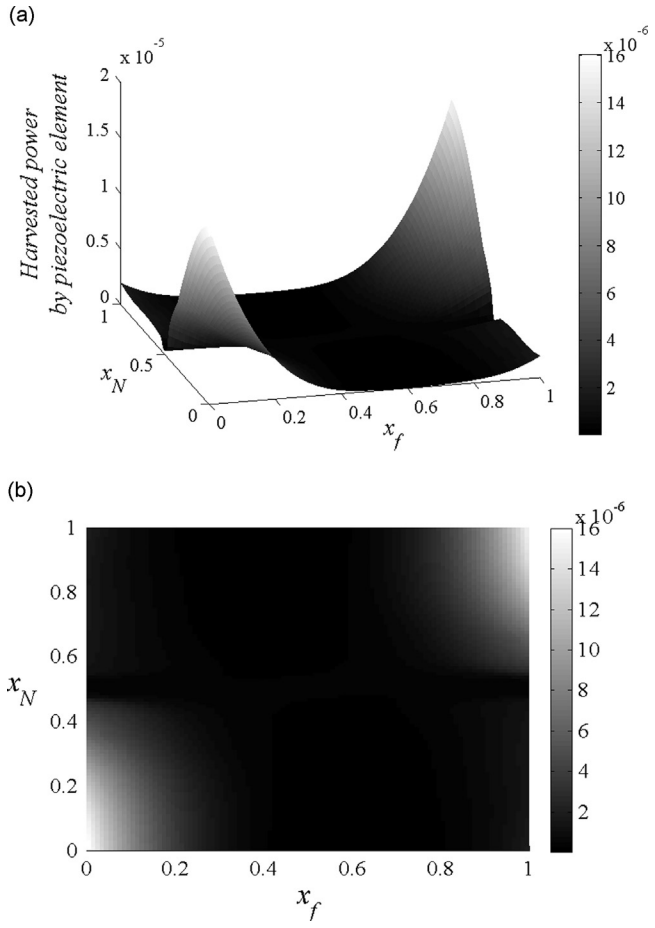

Fig. 8. Harvested power by the piezoelectric element in Configuration♯1 as a function of the NES position and position of load application ($m=1.06, \beta_N=0.47$, $C_p=8.9\mathrm{e}-6$, $\alpha=0.027$, $R=1.1\mathrm{e}+4$, $\varepsilon=0.1, A=10$, $T=0.4/\pi$, $E_BI=291.69$, $M=1.35$, $\beta_1=0.5$, $k_a=1$, $k=100$, $k_p=500$): (a) three-dimensional plot, (b) contour projection in the (x_f, x_N) plane.

approach introduced in [25,26] would be used for this purpose. The optimization problem will be formulated for each configuration separately. For this purpose, the total energy of the beam should be computed. This total energy can be written in the following form for both configurations:

$$\mathrm{TE}(t)=T_b(t)+U_b(t)=\frac{1}{2}E_BI\int_0^L\left(\frac{\partial^2 y(x,t)}{\partial x^2}\right)^2\mathrm{d}x+\frac{1}{2}M\int_0^L\left(\frac{\partial y(x,t)}{\partial t}\right)^2\mathrm{d}x \tag{13}$$

Here the problem of dynamic optimization can be defined as minimization of Eq. (13) subject to system (10) or (11) as follows:

Configuration#1,

$$\min_{m,\ k,\beta_N,x_N,k_p,C_p,\alpha,R}\int_0^t \mathrm{TE}(t)\ \ \mathrm{d}t \tag{14}$$

Subject to Eq. (10)

$$\begin{gathered}
m^{\mathrm{LB}}\le m\le m^{\mathrm{UB}}\\
k^{\mathrm{LB}}\le k\le k^{\mathrm{UB}}\\
{\beta_N}^{\mathrm{LB}}\le\beta_N\le{\beta_N}^{\mathrm{UB}}\\
x_N^{\mathrm{LB}}\le x_N\le x_N^{\mathrm{UB}}\\
{k_p}^{\mathrm{LB}}\le k_p\le{k_p}^{\mathrm{UB}}\\
{C_p}^{\mathrm{LB}}\le C_p\le{C_p}^{\mathrm{UB}}\\
\alpha^{\mathrm{LB}}\le\alpha\le\alpha^{\mathrm{UB}}\\
R^{\mathrm{LB}}\le R\le R^{\mathrm{UB}}
\end{gathered}$$

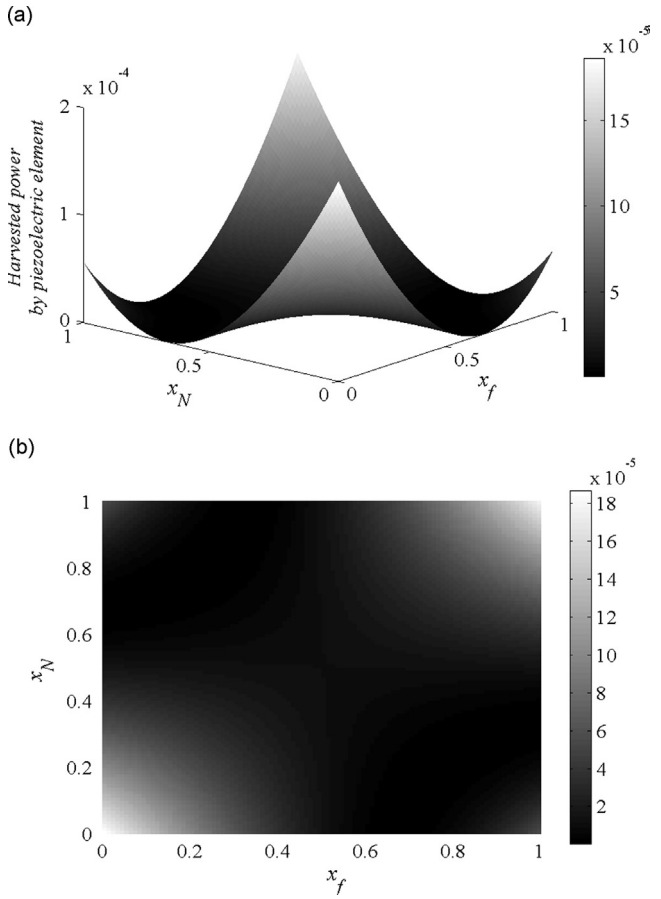

Fig. 9. Harvested power by the piezoelectric element in Configuration#2 as a function of the NES position and position of load application ($m=1.06$, $\beta_N=0.47$, $C_p=8.9\mathrm{e}-6$, $\alpha=0.027$, $R=1.1\mathrm{e}+4$, $\varepsilon=0.1$, $A=10$, $T=0.4/\pi$, $E_BI=291.69$, $M=1.35$, $\beta_1=0.5$, $k_a=1$, $k=420$, $k_p=380$): (a) three-dimensional plot, (b) contour projection in the (x_f, x_N) plane.

Configuration♯2,

$$\min_{m,\ k,\beta_N,x_N,k_p,C_p,\alpha,R} \int_0^t \mathrm{TE}(t)\ \mathrm{d}t \tag{15}$$

Subject to Eq. (11)

$$m^{\mathrm{LB}} \le m \le m^{\mathrm{UB}}$$
$$k^{\mathrm{LB}} \le k \le k^{\mathrm{UB}}$$
$$\beta_N{}^{\mathrm{LB}} \le \beta_N \le \beta_N{}^{\mathrm{UB}}$$
$$x_N^{\mathrm{LB}} \le x_N \le x_N^{\mathrm{UB}}$$
$$k_p{}^{\mathrm{LB}} \le k_p \le k_p{}^{\mathrm{UB}}$$
$$C_p{}^{\mathrm{LB}} \le C_p \le C_p{}^{\mathrm{UB}}$$
$$\alpha^{\mathrm{LB}} \le \alpha \le \alpha^{\mathrm{UB}}$$
$$R^{\mathrm{LB}} \le R \le R^{\mathrm{UB}}$$

Superscripts UB and LB are abbreviations for upper bound and lower bound, respectively.

A Matlab code including fmincon command would be used to obtain the optimized solution. The first step in this code is to initialize the parameter values of the system. Then a set of ordinary-differential equations (Eqs. (10) or (11)) would be solved numerically using ode15s command in Matlab. The results are used to calculate the objective (Eqs. (14) or (15)). Afterward, the fmincon command would be applied to update all parameters. The final step is to check whether the objective is minimum or not. If the objective is minimized, then the optimized set of parameters is obtained and the optimization problem has been successfully solved. Otherwise the updated set of parameters should be used to solve Eq. (10) or (11) again and calculate the objective. This process should be repeated until the optimized set of parameters is achieved.

The portion of the external load energy dissipated through the NES damper and harvested power by the piezoelectric element for both configurations can be obtained using the following relations:

$$P_d(t) \equiv \frac{E_{\mathrm{NES}}}{E_{\mathrm{input\_\ load}}} = \frac{\int_0^t \varepsilon\beta_N \left[\dot{u}(t) - \sum_{r=0}^{\infty} \dot{q}_r(\tau)\Phi_r(x_N)\right]^2 \mathrm{d}\tau}{\int_0^T F(\tau)\sum_{r=0}^{\infty} \dot{q}_r(\tau)\Phi_r(x_f)\mathrm{d}\tau} \tag{16}$$

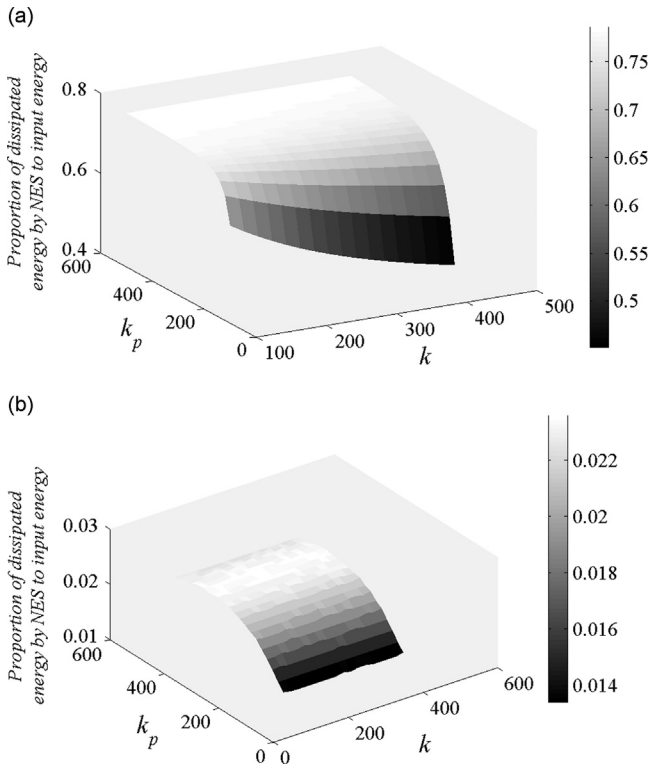

Fig. 10. Contour plots of input energy dissipated by the NES as a function of the piezoelectric element stiffness and the NES spring stiffness ($m=1.06$, $\beta_N=0.47$, $C_p=8.9\mathrm{e}-6$, $\alpha=0.027$, $R=1.1\mathrm{e}+4$, $\varepsilon=0.1$, $A=10$, $T=0.4/\pi$, $E_BI=291.69$, $M=1.35$, $\beta_1=0.5$, $k_a=1$, $x_N=0, x_f=0$): (a) Configuration♯1, and (b) Configuration♯2.

$$P_{hd}(t) = \frac{\text{mean}(V^2)}{R} \tag{17}$$

The limitation in using the dynamic optimization method is its dependency on the choice of initial guess values. This means that if the initial guess is not near enough to the global optimized solution, the method leads to a locally optimized solution. One way to deal with this is to construct a second code, including nested loops, to observe the quality of variations of P_d (or the objective) through changing all parameter values. This can yield better initial guesses. These two codes are applied in parallel to find the optimal solutions. This procedure will be repeated until a globally minimized value for the objective (Eqs. (14) or (15)) is achieved over the selected range for parameter values. The range for each parameter value is chosen wide enough to cover all possible solutions. The globally optimized sets of parameters can be employed in Eq. (16) to obtain the maximum energy dissipated through the NES.

As it will be seen in Section 3, for the present problem, P_d (and so the objective) varies almost uniformly with parameter changes and its variations are somehow predictable. Consequently the method used here to determine the global optimized solution might not be applicable for the functions with unpredictable behavior.

For a small number of parameters, like the problem of this paper, the second code alone would be adequate to obtain the global optimized sets of parameters due to predictability of P_d variations with parameter changes. While for a large number of parameters (in case of having more than one NES and one piezoelectric element attached to the beam), using the second code alone would increase the volume of computations considerably, in this case using both codes in parallel would prevent time-consuming calculations and would increase the method's efficiency.

3. Results and discussion

To compute the transient dynamics of Configurations#1 and 2, the numerical integration of Eqs. (10) and (11) should be performed by considering a finite number of modes. Fig. 3 shows input energy dissipated by the NES as a function of the NES position for Configurations#1 and 2 considering the first 3 modes and the first 5 modes of the system. According to these plots, there is no significant difference between the results obtained by considering the 3 modes and 5 modes. Evidently, the required accuracy for computing the transient dynamics of the systems is attained by considering the first 3 modes. Consequently, just these modes are taken into account for all the forthcoming computations.

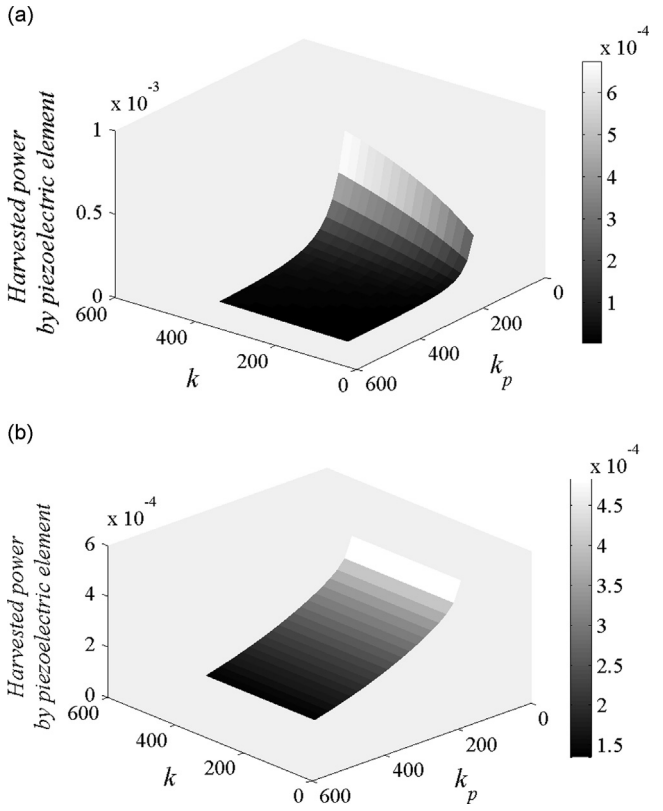

Fig. 11. Contour plots of harvested power by the piezoelectric element as a function of the piezoelectric element stiffness and the NES spring stiffness ($m = 1.06$, $\beta_N = 0.47$, $C_p = 8.9\text{e}{-6}$, $\alpha = 0.027$, $R = 1.1\text{e}{+4}$, $\varepsilon = 0.1$, $A = 10, T = 0.4/\pi$, $E_BI = 291.69$, $M = 1.35$, $\beta_1 = 0.5$, $k_a = 1$, $x_N = 0$, $x_f = 0$): (a) Configuration#1, and (b) Configuration#2.

When the load is applied at $x_f = 0$, the maximum energy dissipation and the maximum harvested power in both configurations are obtained by attaching the NES and the piezoelectric element at $x_N = 0$, as shown in Figs. 3 and 4. Figs. 5–9 depict the influence of the load point application and the NES position on the amount of the dissipated energy and the harvested power. Due to the symmetry, it is enough to just study the first half of the beam.

For Configuration#1, the maximum energy dissipation does not depend on the load point of application for $0 \le x_f \le 0.35$ and it occurs for the NES placed at $x_N = 0$. For the same parameter values, the amount of this maximum would be different for different load points of application (see Fig. 6). In contrast, for $0.36 \le x_f \le 0.5$, the maximum energy dissipation occurs by attaching the NES at a place other than $x_N = 0$ depending on the load point of application. Similarly, the maximum harvested power depends on the load point of application for $0.3 \le x_f < 0.5$.

On the other hand, for Configuration#2, the maximum energy dissipation and the maximum harvested power do not rely on the load point of application and happen for the NES placed at $x_N = 0$ for the first half of the beam.

It is important to note that the dynamic optimization has been performed for the case when the external shock load is applied at $x_f = 0$.

Figs. 10 and 11 show the variations of dissipated energy and harvested power with the system parameters, namely, k_p and k. These figures show that the energy dissipation and the harvested power in Configuration#2 strongly depend on the change in k_p. While for Configuration#1, both k_p and k are influential in variations of dissipated energy and harvested power, increasing k_p would lead to a reduction in harvested power by the piezoelectric element and a rise in dissipated energy by the NES in Configuration#1. In contrast, the result of an increase in k is an increase in harvested power by the piezoelectric element and a reduction in dissipated energy by the NES. However for $k_p \gtrapprox 250$, small changes would occur in the amount of dissipated energy by the NES and harvested power by the piezoelectric element in Configuration#1.

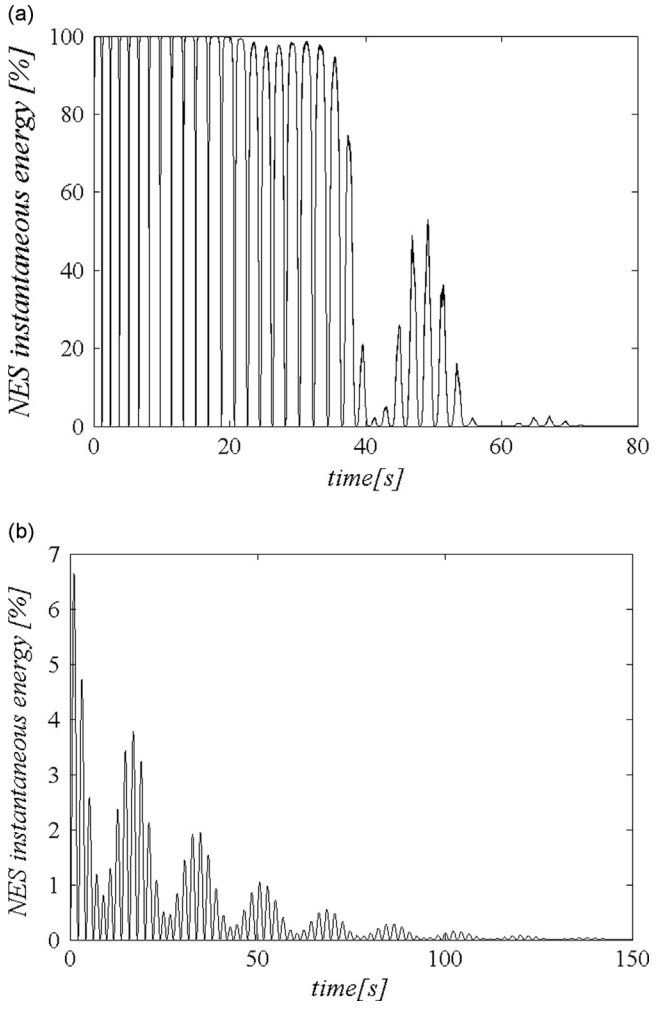

Fig. 12. Instantaneous total energy in the NES of ($m = 1.06$, $\beta_N = 0.47$, $C_p = 8.9\text{e}-6$, $\alpha = 0.027$, $R = 1.1\text{e}+4$, $\varepsilon = 0.1$, $A = 10$, $T = 0.4/\pi$, $E_B I = 291.69$, $M = 1.35$, $\beta_1 = 0.5$, $k_a = 1$, $x_N = 0, x_f = 0$): (a) Configuration#1 for $k = 100$, $k_p = 500$, and (b) Configuration#2 for $k = 420$, $k_p = 380$.

Table 2
Optimized parameters of the system.

	x_N (m)	k (N m^{-1})	m (kg)	β_N (Ns m^{-1})($N\,s\,m^{-1}$)	ε	k_p (N m^{-1})	C_p (F)	α (C m^{-1})	R (Ω)
Configuration#1	0	100	1.06	0.47	0.1	500	8.9e−6	0.027	1.1e+4
Configuration#2	0	420	1.06	0.47	0.1	380	8.9e−6	0.027	1.1e+4

It can be concluded that for Configuration#1, the harvested power by the piezoelectric element has an inverse relationship with the dissipated energy by the NES as varying k_p and k. To illustrate, for the maximum energy dissipation (of 78 percent), the harvested power is minimum. However, there are some regions for which both dissipated energy and harvested power have reasonable high values (e.g., at $k = 160$, $k_p = 140$ where harvested power by piezoelectric element is 1.32×10^{-4} and portion of dissipated energy by the NES is 72 percent).

On the other hand, a significant difference can be observed between the amounts of dissipated energy in these configurations. The maximum energy dissipation in Configuration#1 is 78 percent of the input energy whereas this amount drops to only about 2 percent of the input energy in Configuration#2.

Fig. 12 depicts the instantaneous energy transferred from the beam to the NES. As evidenced in Fig. 12b, the motion localizes to the beam for Configuration#2 and there is no remarkable energy pumping, i.e., only a small amount of energy (of the order of 7 percent) is transferred to the NES in this configuration, while for Configuration#1 this amount rises to about 99 percent. Thus in this configuration almost the entire input energy is passively pumped to the NES and the motion is strongly localized to the NES. Nonlinear characteristics of the system are responsible for this change in dynamics of energy pumping from Configuration#1 to Configuration#2.

As it was demonstrated in [12,27], the dynamics of energy pumping in continuous and discrete systems mainly relie on the topological structures of the nonlinear free periodic solutions (nonlinear normal modes (NNMs)) of the non-dissipative system. Nili Ahmadabadi and Khadem [12] studied in detail the bifurcations and topological structures of NNMs of a cantilever beam attached to a NES. Similar to the present paper, grounded and ungrounded configurations were taken into account and a significant difference was observed between the amounts of the energy transferred to the NES in these configurations. Unlike the grounded configuration, energy pumping occurred effectively in the ungrounded configuration. This was due to the fact that the NNMs corresponding to the grounded configuration were relatively different from those of the ungrounded configuration. In fact, the structures of the NNMs of the grounded configuration were in such a way that made the TET realization impossible.

In this paper, for both configurations, the energy is first confined in the NES and then harvested by piezoelectric element but there is an essential difference between these two configurations. Contrary to Configuration#2, the NES mass in Configuration#1 is attached to the ground via the equivalent stiffness of the piezoelectric layer (k_p). This makes the topological structures of the NMMs to be different for each configuration. For this reason, the energy pumping dynamics is different for each configuration. This also leads to a difference between the amounts of harvested energy by piezoelectric element. In order to obtain more details, a similar approach as the one described in Ref. [12] can be employed to find and evaluate the NNMs of the system. However, this is beyond the scope of this paper and will be addressed in future works.

Table 2 shows the optimized parameters of the system for both configurations. These parameters are obtained using the computer codes explained in Section 2.2.

4. Conclusions

This paper is devoted to design and globally optimize the parameters of a nonlinear energy sink and a piezoelectric-based vibration energy harvester for confining and scavenging vibration energy of a system of free–free beam under shock excitation. Two computer codes were employed in parallel to obtain the globally optimized sets of parameters for nonlinear energy absorber and harvesting system. Two different configurations were examined and the systems' parameters were optimized to both maximize the dissipated energy by the NES and increase the harvested energy by the piezoelectric element. The results indicate that energy pumping occurs effectively in the grounded configuration (Configuration#1) which leads to about 78 percent energy dissipation. Unlike the grounded configuration, there is no remarkable energy transfer to the NES in the ungrounded configuration (Configuration#2).

As far as energy harvesting by piezoelectric element is concerned, satisfactory amount of energy has been harvested as electric power in both configurations.

References

[1] A.F. Vakakis, Inducing passive nonlinear energy sinks in linear vibrating systems, *Journal of Vibration and Acoustics* 123 (2001) 324–332.
[2] O.V. Gendelman, D.V. Gorlov, L.I. Manevitch, A.I. Musienko, Dynamics of coupled linear and essentially nonlinear oscillators with substantially different masses, *Journal of Sound and Vibration* 286 (2005) 1–19.
[3] O.V. Gendelman, A.F. Vakakis, L.I. Manevitch, R. M'Closkey, Energy pumping in nonlinear mechanical oscillators I: dynamics of the underlying Hamiltonian system, *Journal of Applied Mechanics* 68 (2001) 34–41.

[4] O.V. Gendelman, Transition of energy to a nonlinear localized mode in a highly asymmetric system of two oscillators, *Nonlinear Dynamics* 25 (2001) 237–253.
[5] Y. Starosvetsky, O.V. Gendelman, Dynamics of a strongly nonlinear vibration absorber coupled to a harmonically excited two-degree-of-freedom system, *Journal of Sound and Vibration* 312 (2008) 234–256.
[6] A.F. Vakakis, O.V. Gendelman, Energy pumping in nonlinear mechanical oscillators II: resonance capture, *Journal of Applied Mechanics* 68 (2001) 42–48.
[7] Y. Starosvetsky, O.V. Gendelman, Vibration absorption in systems with a nonlinear energy sink: nonlinear damping, *Journal of Sound and Vibration* 324 (2009) 916–939.
[8] Z. Nili Ahmadabadi, S.E. Khadem, Annihilation of high-amplitude periodic responses of a forced two degrees-of-freedom oscillatory system using nonlinear energy sink, *Journal of Vibration and Control* 19 (2013) 2401–2412.
[9] Z. Nili Ahmadabadi, S.E. Khadem, Self-excited oscillations attenuation of drill–string system using nonlinear energy sink, *Proceedings of the Institution of Mechanical Engineers, Part C: Journal of Mechanical Engineering Science* 227 (2012) 230–245.
[10] R. Viguie´, G. Kerschen, J.-C. Golinval, D.M. McFarland, L.A. Bergman, A.F. Vakakis, N. van de Wouw, *Using passive nonlinear targeted energy transfer to stabilize drill-string systems*, *Mechanical Systems and Signal Processing*, 23, , 2009, 148–169.
[11] F. Georgiades, A.F. Vakakis, Dynamics of a linear beam with an attached local nonlinear energy sink, *Communications in Nonlinear Science and Numerical Simulation* 12 (2007) 643–651.
[12] Z. Nili Ahmadabadi, S.E. Khadem, Nonlinear vibration control of a cantilever beam by a nonlinear energy sink, *Mechanism and Machine Theory* 50 (2012) 134–149.
[13] P.J. Cornwell, P.J. Goethal, J. Kowko, M. Damianakis, Enhancing power harvesting using a tuned auxiliary structure, *Journal of Intelligent Material Systems and Structures* 16 (2005) 825–834.
[14] J. Feenstra, J. Granstrom, H.A. Sodano, Energy harvesting through a backpack employing a mechanically amplified piezoelectric stack, *Mechanical Systems and Signal Processing* 22 (2008) 721–734.
[15] E. Lefeuvre, A. Badel, C. Richard, L. Petit, D. Guyomar, A comparison between several vibration-powered piezoelectric generators for standalone systems, *Sensors and Actuators A* 126 (2006) 405–416.
[16] J.Q. Liu, H.B. Fang, Z.Y. Xu, X.H. Mao, X.C. Shen, D. Chen, H. Liao, B.C. Cai, A MEMS-based piezoelectric power generator array for vibration energy harvesting, *Microelectronics Journal* 39 (2008) 802–806.
[17] T.H. Ng, W.H. Liao, Sensitivity analysis and energy harvesting for a self-powered piezoelectric sensor, *Journal of Intelligent Material Systems and Structures* 16 (2005) 785–797.
[18] S.P. Beeby, R.N. Torah, M.J. Tudor, P. Glynne-Jones, T. O'Donnell, C.R. Saha, S. Roy, A micro electromagnetic generator for vibration energy harvesting, *Journal of Micromechanics and Microengineering* 17 (2007) 1257–1265.
[19] S.M. Shahruz, Design of mechanical band-pass filters for energy scavenging:multi-degree-of-freedom models, *Journal of Vibration and Control* 14 (2008) 753–768.
[20] H.A. Sodano, G. Park, D.J. Inman, Estimation of electric charge output for piezoelectric energy harvesting, *Strain* 40 (2004) 49–58.
[21] N.G. Stephen, On energy harvesting from ambient vibration, *Journal of Sound and Vibration* 293 (2006) 409–425.
[22] J.M. Renno, M.F. Daqaq, D.J. Inman, On the optimal energy harvesting from a vibration source, *Journal of Sound and Vibration* 320 (2009) 386–405.
[23] H.A. Sodano, D.J. Inman, A review of power harvesting from vibration using piezoelectric materials, *The Shock and Vibration Digest* 36 (2004) 197–205.
[24] Z. Davis, W. Svendsen, A. Boisen, Design, fabrication and testing of a novel MEMS resonator for mass sensing applications, *Microelectronic Engineering* 84 (2007) 1601–1605.
[25] M. Ouled Chtiba, S. Choura, A.H. Nayfeh, S. El-Borgi, Confinement of vibrations in flexible structures using supplementary absorbers:dynamic optimization, *Journal of Vibration and Control* 16 (2010) 357–376.
[26] M. Ouled Chtiba, S. Choura, A.H. Nayfeh, S. El-Borgi, Vibration confinement and energy harvesting in flexible structures using collocated absorbers and piezoelectric devices, *Journal of Sound and Vibration* 329 (2010) 261–276.
[27] A.F. Vakakis, L.I. Manevitch, O. Gendelman, L. Bergman, Dynamics of linear discrete systems connected to local, essentially non-linear attachments, *Journal of Sound and Vibration* 264 (2003) 559–577.